Multimodal Precipitation in the Superalloy IN738LC

ERCAN BALIKCI and DINC ERDENIZ

IN738LC is a polycrystalline, nickel-base superalloy, which is used in aggressive environments at high temperatures. The required strength is provided by precipitate strengthening. Both unimodal and multimodal precipitate distributions are observed in IN738LC. After reaching a critical size, a unimodal precipitate microstructure transforms to a bimodal one. This transformation is controlled by the precipitate-matrix interface, which is under compression in IN738LC. As the unimodal precipitates grow, the strained interface, due to differential lattice parameter of the matrix and the precipitate phase, stops solute diffusion into the growing precipitates. Hence, the solute atoms, entrapped in the matrix, saturate the matrix and form new, fine precipitates. Dissolution of some large precipitates also supplies solute to supersaturate the matrix. On the other hand, a multimodal precipitate distribution tends to become unimodal at low aging temperatures and bimodal at high aging temperatures. Interestingly, the activation energy is calculated for the coarsening of large precipitates in multimodal distribution and is found to vary with aging time.

DOI: 10.1007/s11661-010-0241-3

I. INTRODUCTION

IN738LC is a nickel-based, polycrystalline cast superalloy, which is used especially in land-based gas turbines. This superalloy has been the sole blade material for electricity producing gas turbines since 1971, and it is still in use with other recently developed alloys.[1] IN738LC was developed in 1969[2] with an intention to combine the mechanical strength expected of high-temperature alloys and especially a good hot corrosion characteristic required in combating the aggressive combustion products.

Superior properties of this material are obtained through strengthening the γ Ni-base matrix solid solution by the γ' $Ni_3(Al,Ti)$ precipitates. MC and $M_{23}C_6$ type carbides also aid in preventing the grain boundary sliding. About 3 vol pct γ-γ' eutectic phase also exists in the structure along with other low melting point boron- and zirconium-based compound phases in a lesser amount.[3,4]

Since performance of this superalloy is strongly influenced by the size and the morphology of the precipitates, microstructural control is extremely important. To this extent, correct knowledge of the phases present in the IN738LC and their transformation behavior is crucial. Differential elemental segregation during solidification into the dendritic and interdendritic regions forms precipitates of different compositions in these regions. In dendritic cores, the precipitates are of aluminum-rich type, whereas those in the interdendritic regions contain more titanium. Dissolution (solvus) temperatures of these two types are naturally different, 1393 K (1120 °C) for the Al-rich precipitates and 1453 K (1180 °C) for the Ti-rich ones.[5,6] A numerical simulation study reports stoichiometric γ' solvus as 1409 K (1136 °C).[7] These suggest that the standard, 2 hours at 1393 K (1120 °C), solution treatment recommended in the literature[8] for this alloy is insufficient for full solutionizing.

Precipitate particles grow obeying the Ostwald ripening, during which precipitate volume fraction increases as solute is rejected by the matrix to the precipitate particles. The precipitates then may grow further at a constant volume fraction, which is called coarsening. Coarsening phenomenon has been formulated by Lifshitz and Slyozov[9] and by Wagner[10] separately, and these two works have been combined into LSW theory. Several other coarsening theories have been suggested based on LSW theory.[11–16] Subsequent to reaching a critical size, precipitates start to dissolve back into the matrix.[17] A full circle of all these stages may be defined as the life cycle of a precipitate.

The precipitate size distribution may be unimodal or multimodal (bimodal, trimodal, *etc*). While a unimodal size distribution is represented by a single Gaussian, a multimodal size precipitate microstructure is composed of distinctly different precipitate size distributions and represented by more than one Gaussian. It has been previously reported[17,18] that the γ' precipitates grow in a unimodal cuboidal morphology up to a critical size, beyond which a bimodal size distribution sets in, where visibly large and small size precipitates coexist. Trimodal precipitate microstructures with large, medium, and small particle sizes have also been reported.[19,20] Significant variations observed in the size of precipitates in such multimodal microstructures points to multiple nucleation stages at different times. While the primary precipitates nucleate and grow during the aging stage and are the large ones in a multimodal microstructure, the medium and small ones are usually believed to nucleate during cooling.

ERCAN BALIKCI, Assistant Professor, and DINC ERDENIZ, MSc Student, are with the Department of Mechanical Engineering, Bogazici University, Istanbul, Turkey. Contact e-mail: ercan.balikci@boun.edu.tr

Manuscript submitted September 17, 2009.
Article published online April 16, 2010

Hence, the precipitates forming during cooling are called "cooling precipitates." Although multimodal precipitate size distribution is usually observed after slow cooling,[7,19–22] an investigation[23] has reported multimodal distribution at intermediate cooling rates. Sarosi *et al.* has also reported multimodal distribution after fast cooling.[22] All these studies have reasoned the formation of multimodal precipitation to the increased diffusion path of the precipitate forming solute elements; as the primary precipitates grow, the space between them increases, which augments the diffusion distance. Hence, the matrix between the precipitate particles becomes supersaturated again, resulting in secondary nucleation, which forms the small precipitates.

In addition to the cooling velocity, alloy composition is also a determining factor in secondary/tertiary nucleation. Influence of the alloy composition to the mode of the final precipitate microstructure has been investigated by Mitchell and Preuss.[20] They have found that aging the superalloy Udimet720 (Special Metals Corp., New Hartford, NY) at 1073 K (800 °C) develops a bimodal distribution subsequent to a subsolvus solution treatment and a unimodal distribution after supersolvus solutionizing. In contrast, the superalloy RR1000 (Rolls-Royce, London, England) forms a bimodal precipitate microstructure after supersolvus solutionizing, which has been reasoned to the presence of tantalum (Ta) in RR1000. As Ta diffuses slower than Al, precipitation of small particles shortens the diffusion path. This same work also shows that small precipitates that start to appear as large precipitates partially dissolve in Udimet720 (Figure 6 in Reference 20).

Growing coherent precipitates may put the interface between the precipitate and matrix under a compressive or tensile stress. When the lattice parameter of the precipitate is larger than that of the matrix, the interface is under compression. The difference in lattice parameter introduces a misfit strain at the interface. The strained interface influences the diffusion of the solute elements in the matrix and toward the precipitates.

This current article discusses the evolution of γ' precipitates in the superalloy IN738LC. An emphasis is given to the mechanisms of multimodal precipitate microstructure formation. Specifically, the aim is to illustrate that such microstructures develop during aging as a result of a strained interface.

II. EXPERIMENTAL PROCEDURE

The material used in this study is a cast, polycrystalline, Ni-base superalloy IN738LC, supplied by Howmet Corporation (Whitehall, MI), in the form of rods, 15 mm in diameter and 110 mm in length. The as-received rods were hot isostatically pressed at 1458 K (1185 °C) for 2 hours in order to remove microporosities and then cooled to room temperature in a neutral atmosphere. After hot isostatic pressing ("hipping"), solution treatment at 1393 K (1120 °C) was conducted for 2 hours; subsequently, an argon-backfill cooling to room temperature was given. An aging treatment at 1116 K (843 °C) was carried out for 24 hours, and cooling to room temperature was performed again by argon backfilling. All these processes were carried out by the supplier. The chemical composition of the as-received stock is given in Table I, and its microstructure consists of a bimodal distribution of irregularly shaped precipitates.[17]

Small, quarter-cylindrical pieces of about 4-mm thickness were cut from the as-received bars for heat treatments, and each of them was sealed in a quartz tube under vacuum at 10^{-3} millibar. Before sealing, the quartz tubes were first vacuumed and then purged 3 times with 99.995 pct purity argon. The samples were individually wrapped with a stainless steel foil in order to prevent reaction with quartz tube. The heat treatments were carried out in a tiltable, tubular furnace, which can reach temperatures up to 1673 K (1400 °C). At the end of a prescribed treatment time, the furnace was tilted, letting the quartz tube drop in a water-filled bucket and the sample to be quenched very quickly.

Since the as-received microstructure was not suitable for the study of the formation and growth of precipitates, the heat treatments started with a solution treatment followed by two sets of aging treatments. In the first set of agings (single agings), the growth of unimodal size precipitates; in the second (double agings), the coarsening behavior of precipitates with a bimodal (fine and coarse) size distribution is analyzed. The heat treatment schedules are given in Table II.

Subsequent to completion of all the heat treatments, samples were prepared for microscopic analysis by metallographic grinding and polishing. They were then etched with a solution containing, by volume, 33 pct HNO_3, 33 pct acetic acid, 33 pct H_2O, and 1 pct HF. A PHILIPS* XL30 ESEM-FEG/EDAX system was used to characterize the size and morphology of the γ' precipitates. A backscattered electron detector was used in the scanning electron microscope (SEM) because of its higher energy and composition sensitivity, giving a good contrast between the matrix (seen as the light background in the microphotographs) and the precipitates, which are the dark regions in the microphotographs. Microphotographs were taken at 15,000, 30,000, 60,000, and 120,000 times magnifications to resolve the extremely fine precipitates, especially in microstructures

*PHILIPS is a trademark of FEI Company, Hillsboro, OR.

Table I. Chemical Composition of the As-Received IN738LC

Element	Ni	Cr	Co	Mo	W	Ta	Nb	Al	Ti	B	Zr	C
Wt pct	balance	15.7 to 16.3	8.0 to 9.0	1.5 to 2.0	2.4 to 2.8	1.5 to 2.0	0.6 to 1.1	3.2 to 3.7	3.2 to 3.7	0.007 to 0.012	0.03 to 0.08	0.09 to 0.13

Table II. Heat Treatment Schedules

Solution Treatment	Aging Treatment	
T/4 h/WQ T = 1508 K(1235 °C), 1523 K(1250 °C), 1573 K(1300 °C)	N/A	
1473 K (1200 °C)/4 h/WQ	1413 K (1140 °C)/t/WQ t = 0.0166, 0.083, 0.166, 0.25, 0.33, 0.5 1393 K (1120 °C)/t/WQ t = 0.25, 0.5, 2, 12, 24 1223 K (950 °C)/t/WQ t = 0.5, 2, 12, 24	Single agings
	1413 K (1140 °C)/4 h/WQ + 1393 K (1120 °C)/t/WQ t = 0.083, 0.166, 0.33,0.5, 4, 12, 24, 48 1413 K (1140 °C)/4 h/WQ + 1223 K (950 °C)/t/WQ t = 1, 3, 6, 12, 24, 48, 96, 240, 480 1413 K (1140 °C)/4 h/WQ + 1023 K (750 °C)/t/WQ t = 4, 12, 48, 240, 480	Double agings

WQ = water quenched, FC = furnace cooled, T = temperature, h = hour, and t = time (h).

with bimodal/trimodal precipitate size distributions. Precipitate sizes were then measured from digital micrographs using the ImageJ image processing software (U.S. National Institutes of Health, Bethesda, MD).[24] The precipitate size reported in this work is an average value of many precipitates in representative microstructural photos. The number of precipitates used in determining the average sizes is given in Table III. Finally, the precipitate size data were analyzed by the linear regression technique; a ''best-fit'' straight line through the data was drawn.

III. RESULTS

Solution treatments, given in Table II, were carried out at four different temperatures for 4 hours followed by fast water quenching. The ones at 1508 K (1235 °C), 1523 K (1250 °C), and 1573 K (1300 °C) produced a supersaturated single-phase solid solution, whereas the one at 1473 K (1200 °C) produced a refined, unimodal precipitate size distribution of about 70 nm, which is in line with previous observations.[17]

Two sets of aging treatments at various temperatures were carried out subsequent to a solution treatment at 1473 K (1200 °C) for 4 hours. The first set of aging treatments was of single agings performed at 1223 K (950 °C), 1393 K (1120 °C), and 1413 K (1140 °C). The microstructures obtained at 1223 K (950 °C) clearly showed a unimodal precipitate size distribution and a coarsening of this unimodal size distribution with increasing aging times. In contrast, a bimodal precipitate microstructure was observed after agings at 1393 K (1120 °C) and 1413 K (1140 °C) within 30 and 10 minutes, respectively. While the large precipitates of the bimodal size distribution were in a continuous growth mode, the small ones seemed not to change their size. These experiments produced data to investigate the size and morphological evolution of the growing precipitates in the early stages of the agings. The size data from the first set of treatments, plotted in Figure 1, were used to obtain the coarsening exponent n in the coarsening equation given as follows:[25]

$$d^n - d_0^n = kt \qquad [1]$$

where t is the time elapsed, k is the coarsening rate constant, d_0 is the precipitate size at time zero, and d is the size at time t.

The second set of aging treatments was designed to investigate the evolution of the small and large precipitates in the bimodal microstructure. In these, the specimens first were given an aging at 1413 K (1140 °C) for 4 hours to produce the bimodal size distribution with ~50 nm round small and ~450 nm cuboidal large precipitates, and then a second aging was performed at three different temperatures (1023 K (750 °C), 1223 K (950 °C), and 1393 K (1120 °C)) to observe the progress of both the small and large precipitates at these aging temperatures. Especially, the temperatures of 1023 K (750 °C) and 1223 K (950 °C) are relevant to working temperatures of this superalloy (IN738LC) in gas turbines.[1] For specimens treated at 1023 K (750 °C), no change in the size of the large or small precipitates could be measured. However, both the small and large precipitates grew at 1223 K (950 °C) in time. Although the size difference between the small and large precipitates slightly decreased, a single size distribution was not obtained even after 480 hours of aging at 1223 K (950 °C). Interestingly, a trimodal (small, medium, and large) precipitate size distribution was observed at 1393 K (1120 °C) after agings up to 4 hours, as seen in a representative microphotograph in Figure 2. As the medium and large size precipitates grew at 1393 K (1120 °C), the small ones kept their size unchanged. Indeed, the faster growth of the medium size precipitates than that of the coarse ones enabled the transformation of the trimodal size distribution to a bimodal size distribution in 4 hours. Besides, it is worth mentioning that the cuboidal morphology of the coarse precipitates degenerated into a noncuboidal one beyond 12 hours of secondary agings at 1393 K (1120 °C). The size data produced *via* the second set of treatments were plotted in

Table III. Number of Precipitates Used in Determining the Average Precipitate Size

T	t	0.083	0.166	0.25	0.33	0.5	1	2	3	4	6	12	24	48	96	240	480
1223 K (950 °C)		—	—	—	—	128	—	79	—	—	—	105	80	—	—	—	—
1393 K (1120 °C)		—	—	112	—	62	—	225	—	—	—	75	61	—	—	—	—
1413 K (1140 °C)		47	60	44	33	22	—	—	—	—	—	—	—	—	—	—	—
1413 K (1140 °C) +	1023 K (750 °C)	—	—	—	—	—	—	—	—	125		104		86		108	77
	1223 K (950 °C)	—	—	—	—	—	152 (5455)		158 (12053)		56 (975)	83 (827)	158 (821)	161 (313)	83 (786)	142 (112)	34 (19)
	1393 K (1120 °C)	151 (51)	22 (53)		143 (56)	83 (75)	—	—	—	133		43	39	43	—	—	—

T = aging temperature and t = aging time in hours. Value in each cell is the number of precipitates at a T-t combination. Values in parentheses are for small precipitates in bimodal/trimodal microstructures.

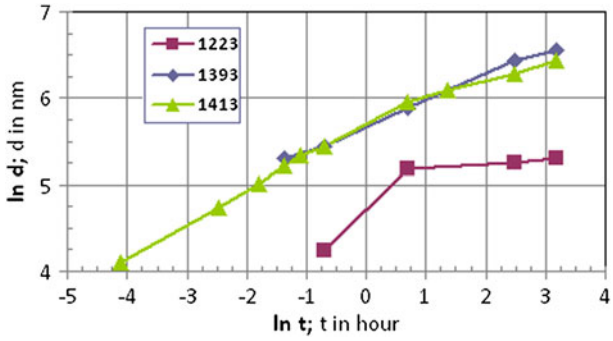

Fig. 1—Logarithmic precipitate size *vs* aging time for three single aging temperatures. Slopes of the lines yield the coarsening exponent. Last four data points at 1413 K (1140 °C) are from Ref. 18.

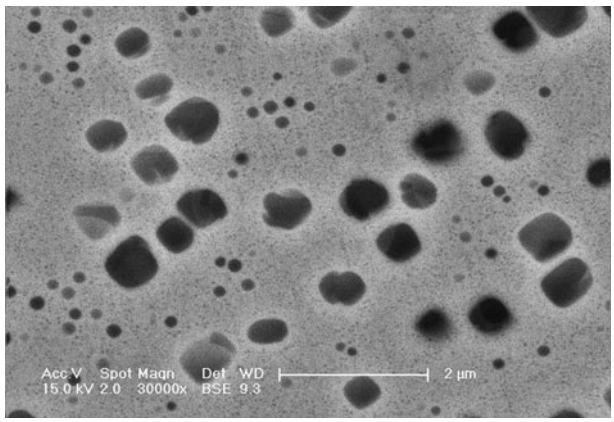

Fig. 2—Trimodal precipitate size distribution obtained after double aging of 1413 K (1140 °C)/4 h/WQ + 1393 K (1120 °C)/10 min/WQ. Very fine, small precipitates are seen in the background. Medium and large size precipitates are more visible.

Figure 3, which helped determine the coarsening exponent n and the coarsening activation energy Q.

IV. DISCUSSION

A. *Solution Treatments*

Commercial heat treatments for superalloys generally consist of two steps: solutionizing and aging. Full solutionizing is necessary for a controlled development of a desired precipitate microstructure during aging. The standard heat treatment suggested[2] for the IN738LC starts with a solution treatment at 1393 K (1120 °C), which is a subsolvus temperature and obviously not adequate for dissolution of at least the interdendritic precipitates.[5,6] It has been reported by Balikci *et al.*[17] that full solutionizing of the IN738LC occurs at and above 1508 K (1235 °C). However, from the property degradation point of view, a solution treatment at 1508 K (1235 °C) may be deleterious if the treatment is not carried out carefully, considering the fact that low melting point phases display incipient melting above 1393 K (1120 °C).[5] Nevertheless, a stepwise, slow heating above 1508 K (1235 °C) may dissolve the low

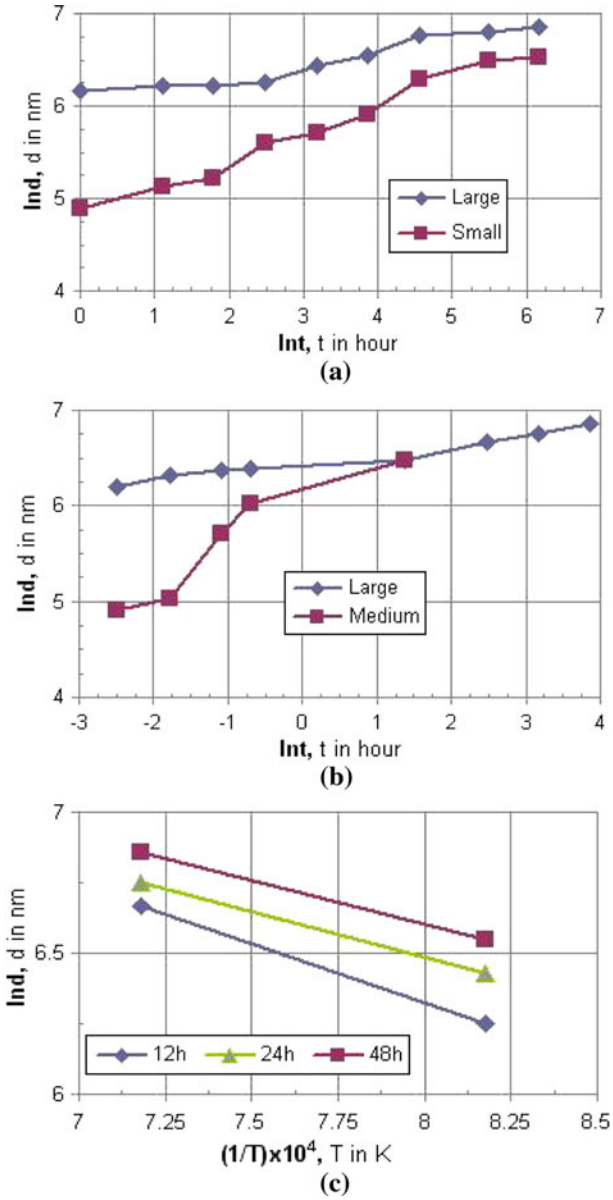

Fig. 3—Logarithmic precipitate size *vs* aging time for double agings (*a*) at 1223 K (950 °C) and (*b*) at 1393 K (1120 °C). Slopes of the lines yield the coarsening exponent. Ln *d vs* $1/T$ plots (*c*) help determine the coarsening activation energy.

melting phases, together with the γ' precipitates, into the matrix but prevent incipient melting.[26]

The solution treatments (Table II) have been carried out in the current study to double check the results obtained previously[17] and to further investigate if the precipitation in the superalloy IN738LC is a result of a nucleation/growth or spinodal decomposition process. Incipient melting was not the focus of the present treatments. Henderson and McLean[27] report that solution treatment at 1473 K (1200 °C) is sufficient to dissolve precipitates completely, but they reform as very fine particles during cooling. Similar fine precipitate microstructure is also observed after the solution treatment at 1473 K (1200 °C) in the present study. In fact, this temperature is very close to the hipping temperature 1458 K (1185 °C) of the superalloy IN738LC after casting. Hence, 1393 K (1120 °C) given as the standard solution treatment temperature is actually the first aging temperature for the superalloy IN738LC, and the aging at 1123 K (850 °C) for 24 hours is the secondary aging. All these steps (hipping and double agings) produce a bimodal distribution of irregularly shaped precipitates.[17] In contrast, a single-phase solid solution obtained in the present study after solution treatments at and above 1508 K (1235 °C) substantiates the fact that the precipitation can be inhibited, which is contrary to the understanding that the precipitation cannot be suppressed in a spinodal decomposition process during cooling as it requires no activation energy barrier. It should be noted, however, that the microstructural characterizations in the current work have been conducted with a field emission gun–scanning electron microscope (FEG-SEM); thus, all the microstructural observations have been obtained within the limits of the FEG-SEM with 2-nm resolution. Additionally, research conducted by Rosen *et al.*[28] provides concrete support of this idea. They have used a four-point probe arrangement to determine resistivity changes during aging of an already solution-treated, γ' precipitate forming alloy. They have recorded an increase in electrical resistivity, which is a sign for short-range ordering of atoms, namely, formation of γ' precipitates. This shows that precipitation is a result of normal nucleation and growth processes rather than spinodal decomposition. If it were the spinodal, no resistivity increase would be observed since the precipitates would have formed already during solution quenching. Rather, a continuous decrease in resistivity would be measured as precipitates coarsened and led to an increase in the mean free path for electrons.

B. *Single Agings at 1223 K (950 °C), 1393 K (1120 °C), and 1413 K (1140 °C)*

Total internal energy of a precipitate microstructure is determined by the volume, interfacial area, and strain energy terms;[25] minimization of this energy leads to a stable microstructure. For a given volume, energy contribution from the interfacial surfaces decreases as the precipitates grow. Nevertheless, a lattice mismatch between a coherent precipitate and its matrix introduces an additional increase in the internal energy of the material as precipitates grow. However, the mismatch can be minimized for the cubic crystal systems by matching the {100} surfaces of the precipitates and the matrix. This match actually reduces the surface energy contribution as well, since the {100} surfaces are low energy planes, for example, in face-centered-cubic (fcc) crystals.[25,29] Note that the matrix in IN738LC is in conventional fcc, while the γ' precipitate phase is in ordered fcc structure. Furthermore, γ' precipitates in the superalloy IN738LC display a small (0.38 pct), positive lattice mismatch with the matrix.[30] Hence, driven by a reduction in total internal energy, a morphological transformation from a spheroidal to a cuboidal shape is usually observed for growing, coherent γ' precipitates, where the cube faces are {100} planes.

The single aging treatments in the current study have shown that such a transformation takes only 10 minutes at 1413 K (1140 °C). A previous study has shown longer transformation times, *e.g.*, 24 hours at 1323 K (1050 °C) and more than 24 hours at 1223 K (950 °C).[17] Of course, this trend is expected because at higher temperatures the kinetics is faster; so is the transformation.

The formation of a bimodal precipitate microstructure in specimens single aged at 1393 K (1120 °C) and 1413 K (1140 °C) signals to the conventional suggestion that the fine precipitates form during quenching as solubility decreases with decreasing temperature. Such precipitates are named "cooling precipitates." Multiple nucleation may also take place during cooling, resulting in a multimodal precipitate microstructure.[25] As the primary precipitates grow, spacing between them increases, which results in the supersaturation of the matrix between them because the diffusion path for the precipitate forming solute atoms increases. Hence, the secondary or tertiary precipitates can form between the large precipitates.[19–23]

Nonetheless, another mechanism for the formation of fine secondary/tertiary precipitates may be plausible; the fine precipitates might already exist at the aging temperature. It is reasonable to think that the growth of large, coherent precipitates becomes extremely sluggish[31] and cannot be sustained beyond a critical size due to enormously increased mismatch strain energy.[17,30] Besides, kinetic calculations have previously shown increased activation energy for precipitate growth with increased unimodal precipitate size, which verifies deceleration of precipitate coarsening.[17] In addition, a positive misfit that exists in the superalloy IN738LC[30] puts the interface under a compressive stress.[29] Hence, the strained interface may prevent solute diffusion to the precipitates for their growth, which keeps the solute atoms in the matrix. In fact, the coarsening of the precipitates is already stated by Ardell and Ozolins to be interface controlled.[32] Thus, the precipitate formers remaining in the matrix can resaturate the matrix to form fine precipitates for which the lattice mismatch is insignificant.[29] Also, the strained, solute-free zones may lead to the formation of precipitate denuded zones around already coarse ones, as observed in the current (light zones around large precipitates in Figure 2) and previous studies.[17] The fine precipitates are absent at 1393 K (1120 °C) and 1413 K (1140 °C) after short agings (up to 10 and 30 minutes, respectively) and especially when the superalloy is aged at 1223 K (950 °C) for times from 30 minutes up to 24 hours followed by quenching. (Microstructures have been analyzed by SEM with magnifications up to 120,000 times.) This indicates that the solute remaining in the matrix cannot precipitate out as fine ones either during aging or during quenching. That is because the growing precipitates are not large enough to critically strain the interface to prevent solute diffusion into the growing precipitates and so to supersaturate the matrix again.

It should be noted that the interfacial strain that can develop at a given temperature will depend on the precipitate size and also on the differential thermal expansions of the matrix and the precipitate phases at the temperature of interest.[33] The present study shows that a bimodal microstructure ensues after 10 minutes at 1413 K (1140 °C) when the large precipitate size is about 151 nm, which is comparable to the 229 nm that forms in 30 minutes at 1393 K (1120 °C). Obviously, a transmission electron microscopy analysis can determine with a better accuracy the critical precipitate size required for the formation of a bimodal microstructure. In addition, although bulk thermal expansion of IN738LC with various precipitate microstructures have already been determined,[33] a study elucidating the individual thermal expansion of the precipitate and matrix phases in the constrained condition may help understand the magnitude of the interfacial strain. It is interesting to note that a very large precipitate size (9 μm) is reached before the bimodal microstructure formation at 1373 K (1100 °C).[34] On the contrary, it takes only 1 second at 1433 K (1160 °C) to split the unimodal size, 700-nm coarse cuboidal precipitates into 70-nm fine precipitate particles.[35] Thus, longer aging times than 24 hours conducted in this study at 1223 K (950 °C) may also lead to a bimodal precipitate size distribution at this temperature. As a result, the fine precipitates observed in multimodal microstructures may possibly form at a given aging temperature only when the coherent large ones mature enough to strain the interface, preventing further solute diffusion into the large precipitates.

C. *Double Agings at 1023 K (750 °C), 1223 K (950 °C), and 1393 K (1120 °C)*

The second aging at 1023 K (750 °C), subsequent to the first aging at 1413 K (1140 °C), has no effect on the bimodal size distribution, perhaps because of low thermal energy available at this low temperature. In fact, an extremely sluggish precipitate growth in IN738LC at temperatures of 923 K (650 °C) and 1023 K (750 °C) has already been reported by Balikci *et al.*[17] Furthermore, a study reports through a comparable aging treatment the presence of the fine precipitates even after 3000 hours.[31] On the other hand, when a bimodal precipitate microstructure, produced *via* the first aging at 1413 K (1140 °C), is aged at 1223 K (950 °C), it is observed that the precipitate size evolves toward a unimodal size distribution in time, as seen in Figure 3(a), although a fully unimodal distribution has not been observed after 480 hours. Nevertheless, during the second aging at 1393 K (1120 °C), the trimodal size distribution (Figure 2) has been transformed to the bimodal size distribution in 4 hours (Figure 3(b)). This transformation has taken place *via* a faster growth rate of the medium size precipitates than that of the large ones, which enabled the medium ones to catch the large ones in 4 hours. Of course, this process has diminished the medium ones, whereas the small ones have replenished and not changed their size, probably through the corner dissolution mechanism.[17] It may be possible that the matrix is not yet strained critically during the first few minutes of the second aging at 1393 K (1120 °C). Hence, some of the fine precipitates already formed after first aging (at 1413 K (1140 °C)) can merge and coarsen, which results in trimodal size distribution. Besides, it is

Table IV. Coarsening Exponent and Correlation Coefficients

Aging	n_L	n_S
1223 K (950 °C)	3.45*/4.03 (R^2 = 0.984*/0.732)	
1393 K (1120 °C)	3.46 (R^2 = 0.996)	
1413 K (1140 °C)	3.13 (R^2 = 0.975)	
1413 K (1140 °C) + 1223 K (950 °C)	7.62 (R^2 = 0.926)	3.43 (R^2 = 0.980)
1413 K (1140 °C) + 1393 K (1120 °C)	10.76 (R^2 = 0.960)	1.52** (R^2 = 0.926)

n_L: Coarsening exponent for large precipitates.
n_S: Coarsening exponent for small/medium precipitates.
*This value is obtained by omitting the second data point in the data series at 1223 K (950 °C).
**This value is calculated for the coarsening of medium precipitates of the trimodal microstructure observed at 1393 K (1120 °C).

worth mentioning that the cuboidal morphology of the coarse precipitates has degenerated to a noncuboidal one beyond 12 hours of secondary agings at 1393 K (1120 °C) as a result of the corner dissolution.[17] This degeneration supplies solute to the matrix for the cyclic formation of fresh, fine precipitates.

D. *Kinetics*

The logarithmic form of Eq. [1] establishes a linear relationship between the precipitate size and aging time. Figure 1 shows this correlation by the ln *d vs* ln *t* plots for the size data obtained up to 24 hours. Correlation coefficients and growth exponents obtained by using these plots are tabulated in Table IV. Additional data points at 1413 K (1140 °C) after 30 minutes up to 24 hours are used from an earlier work.[18] A highly linear correlation, pointed out by the *R*-squared values of the first set of aging treatments at 1223 K (950 °C), 1393 K (1120 °C), and 1413 K (1140 °C), indicates the applicability of Eq. [1] to the superalloy IN738LC. The coarsening exponent values are very close to 3, which is the generally reported coarsening exponent for superalloys. It should be noted that inclusion of all the data at 1223 K (950 °C) does not produce a perfectly linear correlation; the R^2 value is 0.732. However, the value increases to 0.984 when the second data point is excluded. This omission is only suggested because the relationship becomes linear; otherwise, the suggestion is not based on any error analysis procedure. Indeed, it may require multiple aging treatments to establish the magnitude of an experimental error, but only one aging treatment was carried out at 1223 K (950 °C) for the second data point (2 hours).

During double agings, both the large and small precipitates grow. The growth exponents determined for the second agings both at 1223 K (950 °C) and 1393 K (1120 °C) indicate that the large precipitates grow slower than the fine precipitates, so the microstructure evolves a unimodal precipitate size distribution (Figure 3). This is, in fact, implied by the time derivative of Eq. [1].[25] It should be remembered, however, that the microstructure at 1393 K (1120 °C) consists of a trimodal precipitate size distribution, and the medium size precipitates, in fact, grow very fast (n = 1.52, Table IV) to the size of the large precipitates and so disappear in 4 hours (Figure 3(b)).

The activation energy for coarsening of the large precipitates in the bimodal distribution has been calculated again by using Eq. [1] in which k is taken as $k_o e^{-Q/RT}$, where k_o is a constant, Q is the activation energy, R is the gas constant, and T is the absolute temperature. The slopes of the ln d *vs* $1/T$ plots, as seen in Figure 3(c), have been used in the calculations. Interestingly, the activation energy is found to vary with aging time and is calculated to be the highest (317 kJ/mol) for the 12-hour treatments and the lowest (234 kJ/mol) for the 48-hour treatments. The 24-hour treatments give an intermediate value of 246 kJ/mol. This finding, in line with that reported by Roy *et al.*,[37] shows that the coarsening becomes easier with longer aging time. This and the previous observations documented in the literature[36] suggest that activation energy is not constant but varies through different regimes of precipitate evolution.

V. CONCLUSIONS

1. Full solutionizing is achieved at and above 1508 K (1235 °C).
2. A unimodal precipitate size distribution evolves into a bimodal size distribution when the growing precipitates attain a critical size. This transformation is claimed to be a result of strained precipitate/matrix interface. Such an interface prevents solute diffusion into the growing precipitates. Thus, the precipitate forming solute atoms entrapped in the matrix eventually supersaturate the matrix and form fresh fine precipitates. Partial dissolution of large precipitates can also provide solute for supersaturating the matrix.
3. A multimodal size distribution evolves toward a unimodal one at low aging temperatures 1223 K (950 °C) and toward a bimodal at high temperatures 1393 K (1120 °C).
4. Calculated growth exponent for the unimodal precipitate size distribution is nearly the same as that generally reported for superalloys. In the case of the multimodal size distribution, however, it is found that the small or medium size precipitates grow faster than the large ones. As a result, a bimodal distribution transforms to a unimodal one and a trimodal distribution transforms to a bimodal one.
5. Calculated coarsening activation energy for coarse precipitates in a multimodal distribution is found to vary with aging time.

ACKNOWLEDGMENTS

The authors appreciate the financial support provided by Bogazici University Scientific Research Projects (BAP) through Grant No. 05HA601. EB also acknowledges with gratitude the help in aging treatments by undergraduate senior student Mr. Mustafa

Sengor and in metallography by MSc student Mr. Daghan Arpaci.

REFERENCES

1. P.W. Schilke: GER 3569G, GE Energy Report, "Advanced Gas Turbine Materials and Coatings", New York, NY, 2004.
2. C.G. Bieber and J.J. Galka: U.S. Patent No. 3,459,545, Aug. 5, 1969.
3. R.K. Sidhu, O.A. Ojo, and C.M. Chaturvedi: *Metall. Mater. Trans. A*, 2007, vol. 38A, pp. 858–70.
4. O.A. Ojo, N.L. Richards, and M.C. Chaturvedi: *Metall. Mater. Trans. A*, 2006, vol. 37A, pp. 421–33.
5. O.A. Ojo, N.L. Richards, and M.C. Chaturvedi: *Mater. Sci. Technol.*, 2004, vol. 20, pp. 1027–34.
6. R. Roshental and D.R.F. West: *Mater. Sci. Technol.*, 1994, vol. 15, pp. 1387–94.
7. S. Behrouzghaemi and R.J. Mitchell: *Mater. Sci. Eng. A*, 2008, vol. 498, pp. 266–71.
8. C.G. Bieber and J.R. Mihalisin: *2nd Int. Conf. on the Strength of Metals and Alloys*, Pacific Grove, CA, 30 Aug–4 Sept 1970, The American Society for Metals, Metals Park, Ohio, 1970.
9. I.M. Lifshitz and V.V. Sloyozov: *J. Phys. Chem. Solids*, 1961, vol. 19 (1–2), pp. 35–50.
10. C. Wagner: *Z. Elektrochemie*, 1961, vol. 65 (7–8), pp. 581–91.
11. A.J. Ardell: *Acta Metall.*, 1972, vol. 20 (1), pp. 61–71.
12. A.D. Brailsford and P. Wynblatt: *Acta Metall.*, 1979, vol. 27 (3), pp. 489–97.
13. C.K.L. Davies, P. Nash, and R.N. Stevens: *Acta Metall.*, 1980, vol. 28 (2), pp. 179–89.
14. K. Tsumuraya and Y. Miyata: *Acta Metall.*, 1983, vol. 31 (3), pp. 437–52.
15. J.A. Marqusee and J. Rose: *J. Chem. Phys.*, 1984, vol. 80 (1), pp. 536–43.
16. P.W. Voorhees and M.E. Glicksman: *Acta Metall.*, 1984, vol. 32 (11), pp. 2001–11.
17. E. Balikci, A. Raman, and R.A. Mirshams: *Metall. Mater. Trans. A*, 1997, vol. 28A, pp. 1993–2003.
18. E. Balikci, R.A. Mirshams, and A. Raman: *Z. Metallkd.*, 1999, vol. 90 (2), pp. 132–40.
19. R.J. Mitchell, M. Preuss, M.C. Hardy, and S. Tin: *Mater. Sci. Eng. A*, 2006, vol. 423, pp. 282–91.
20. R.J. Mitchell and M. Preuss: *Metall. Mater. Trans. A*, 2007, vol. 38A, pp. 615–27.
21. J. Mao, K. Chang, W. Yang, K. Ray, S.P. Vaze, and D.U. Furrer: *Metall. Mater. Trans. A*, 2001, vol. 32A, pp. 2441–49.
22. P.M. Sarosi, B. Wang, J.P. Simmons, Y. Wang, and M.J. Mills: *Scripta Mater.*, 2007, vol. 57, pp. 767–70.
23. Y.H. Wen, J.P. Simmons, C. Shen, C. Woodward, and Y. Wang: *Acta Mater.*, 2003, vol. 51, pp. 1123–32.
24. W.S. Rasband: Image J, U.S. National Institutes of Health, Bethesda, MD, http://rsb.info.nih.gov/ij/, 1997–2007.
25. D.A. Porter and K.E. Easterling: *Phase Transformations in Metals and Alloys*, 2nd ed., Chapman and Hall, New York, NY, 1992, pp. 112, 265, 315, and 316.
26. M. Durand-Charre: *The Microstructure of Superalloys*, Gordon and Breach Science Publishers, Amsterdam, 1997, pp. 68–69.
27. P.J. Henderson and M. McLean: *Acta Metall.*, 1983, vol. 31 (8), pp. 1203–19.
28. G.I. Rosen, S.F. Dirnfeld, M. Bamberg, and B. Prinz: *Z. Metallkd.*, 1994, vol. 85, pp. 127–30.
29. P.K. Footner and B.P. Richards: *J. Mater. Sci.*, 1982, vol. 17, pp. 2141–53.
30. E. Balikci, R.E. Ferrell, Jr., and A. Raman: *Z. Metallkd.*, 1999, vol. 90, pp. 141–46.
31. R.S. Moshtaghin and S. Asgari: *Mater. Des.*, 2003, vol. 24, pp. 325–30.
32. A.J. Ardell and V. Ozolins: *Nat. Mater.*, 2004, vol. 4, pp. 309–16.
33. E. Balikci, A. Raman, and R.A. Mirshams: *Metall. Mater. Trans. A*, 1999, vol. 30A, pp. 2803–08.
34. K. Dwarapureddy, E. Balikci, S. Ibekwe, and A. Raman: *J. Mater. Sci.*, 2008, vol. 43 (6), pp. 1802–10.
35. E. Balikci and A. Raman: *J. Mater. Sci.*, 2000, vol. 35 (14), pp. 3593–97.
36. E. Balikci and A. Raman: *J. Mater. Sci.*, 2008, vol. 43, pp. 927–32.
37. I. Roy, E. Balikci, S. Ibekwe, and A. Raman: *J. Mater. Sci.*, 2005, vol. 40, pp. 6207–15.